ANTIOXIDANTS & REDOX SIGNALING
Volume 20, Number 13, 2014

DOI: 10.1089/ars.2013.5737

NEWS & VIEWS

Does *Uncoupling Protein 2* Expression Qualify as Marker of Disease Status in *LRRK2*-Associated Parkinson's Disease?

Anne Grünewald,[1,2] Björn Arns,[1] Britta Meier,[1] Kathrin Brockmann,[3,4] Vera Tadic,[1] and Christine Klein[1]

Abstract

Mutations in *leucine-rich repeat kinase 2* (*LRRK2*) are the most common known genetic cause of late-onset Parkinson's disease (PD). However, the penetrance of the disease is below 50% at 60 years of age. LRRK2 is associated with the mitochondrial membrane, and mutant forms impair the function of the organelle and autophagosome clearance in human cells, including induced pluripotent stem cell-derived neurons. Elevated expression of uncoupling proteins has been identified as the cause of mitochondrial depolarization in human fibroblasts with G2019S LRRK2. To identify factors that contribute to the penetrance of *LRRK2* mutations, we studied respiratory chain function, markers of mitochondrial uncoupling, oxidative stress, and autophagy in fibroblasts from affected and unaffected carriers of the G2019S mutation. Independent of disease status, all mutation carriers showed reduced mitochondrial membrane potential, increased proton leakage, and more fragmented mitochondria. However, a significant increase in the expression of *uncoupling protein 2* (*UCP2*) was only detected in affected individuals with the G2019S mutation in LRRK2. Since oxidative stress and autophagic markers were selectively increased in some of the PD patients, we hypothesize that *UCP2* expression is upregulated in response to elevated reactive oxygen species generation in affected mutation carriers and that *UCP2* mRNA levels might, therefore, serve as markers of disease status in *LRRK2*-associated PD. *Antioxid. Redox Signal*. 20, 1955–1960.

Introduction

MUTATIONS IN *leucine-rich repeat kinase 2* (*LRRK2*) are the most frequently known genetic cause of late-onset autosomal dominant Parkinson's disease (PD) (3). *LRRK2*-mutant patients present with a phenotype similar to that of idiopathic cases (6). However, the cumulative risk for carriers of *LRRK2* mutations to develop PD is only between 51% and 64% at 69 years of age, depending on the mutation type (3). A large number of mutation-positive individuals do not develop a motor phenotype despite a latent dopaminergic deficit (1).

LRRK2 encodes a multimodal protein containing an Ras-like GTP binding domain and a serine, threonine kinase domain. The most common LRRK2 mutation, G2019S, is situated within the latter domain, increasing the kinase activity and toxicity of the protein. LRRK2 is not only mainly localized in the cytoplasm but also associated with membranous structures, including mitochondria (2). In keeping with these findings, G2019S-mutant LRRK2 has been shown to impact mitochondrial function and morphology in PD patient fibroblasts (4). A decrease in mitochondrial membrane potential is associated with elevated mRNA expression of *uncoupling proteins (UCP) 2* and *4* in fibroblasts with G2019S LRRK2 or SHSY5Y cells over-expressing G2019S LRRK2, respectively (6).

Identified mitochondrial phenotypes in LRRK2-associated PD link the protein to the well-described PINK1-Parkin

[1]Institute of Neurogenetics, University of Lübeck, Lübeck, Germany.
[2]Wellcome Trust Centre for Mitochondrial Research, Institute of Ageing and Health, Newcastle University, Newcastle upon Tyne, United Kingdom.
[3]Department of Neurodegenerative Diseases, Hertie-Institute for Clinical Brain Research, Tübingen, Germany.
[4]Graduate School for Cellular and Molecular Neuroscience, University of Tübingen, Tübingen, Germany.

Innovation

Mutations in *leucine-rich repeat kinase 2* (*LRRK2)* are the most common genetic cause of Parkinson's disease despite their relatively low penetrance. To date, the factors influencing penetrance remain mostly elusive. In this study, we showed that the gene expression of the mitochondrial uncoupler *uncoupling protein 2 (UCP2)* is significantly increased in affected individuals harboring the G2019S mutation, whereas unaffected carriers of the same mutation show normal *UCP2* mRNA concentrations. In light of elevated protein levels of oxidative stress and autophagic markers, we hypothesize that the strong upregulation of *UCP2* in affected mutation carriers is a sign of overburdening of the cellular reactive oxygen species scavenging system in these individuals.

mitophagy pathway. Mutations in *PINK1* or *Parkin* cause recessive PD and trigger an accumulation of dysfunctional mitochondria in neuronal and non-neuronal cellular systems (9). Similarly, G2019S-mutant LRRK2 compromises autophagosome clearance in human induced pluripotent stem cell (iPSC)-derived dopaminergic neurons (8).

To detect potential markers of disease status (or even disease manifestation) and compensating factors in *LRRK2*-associated PD, we investigated mitochondrial function and autophagy phenotypes in fibroblasts from PD patients and unaffected carriers of the G2019S mutation. This approach identified *UCP2* expression as a potential marker of disease status in *LRRK2*-associated PD.

Results

Reduced mitochondrial membrane potential and interconnectivity in PD patients and unaffected carriers with G2019S mutation

First, we assessed the mitochondrial membrane potential in fibroblasts from affected and unaffected individuals harboring the G2019S mutation in LRRK2 as well as mutation-negative healthy controls. This measurement resulted in a significant reduction in mutation-positive individuals independent of their disease status ($p_{unaffected} < 0.05$ and $p_{affected} < 0.01$; Fig. 1A). Investigation of oxygen consumption rates (OCRs) using an extracellular flux analyzer showed comparable levels in all individuals under basal conditions (Fig. 1B). Determination of the OCRs after oligomycin treatment enables an indirect measure of the proton leak through the inner mitochondrial membrane in the cells (6). This analysis revealed significantly increased uncoupling of the respiratory chain in fibroblasts of all mutation-positives ($p < 0.001$; Fig. 1C). By contrast, the maximum respiration determined after exposure to the ionophore FCCP was not altered in the mutants (Fig. 1D). In support of our results pointing toward increased uncoupling in individuals with the G2019S mutation in LRRK2, determination of mitochondrial interconnectivity by calculation of the form factor revealed more fragmentation in these cases ($p_{unaffected} < 0.01$ and $p_{affected} < 0.05$; Fig. 1E). Furthermore, the integrity and copy number of the mitochondrial genome (mtDNA) was studied. In terms of mtDNA lesions, no differences between the investigated groups were determined. Conversely, the mitochondrial copy number was slightly elevated in unaffected mutation carriers ($p < 0.01$) and decreased in affected mutation carriers ($p < 0.01$) (Fig. 1F).

mRNA expression of UCP2 *is elevated in affected G2019S LRRK2 mutant cases*

To determine the cause of the observed mitochondrial uncoupling in G2019S LRRK2-mutant fibroblasts, we quantified the expression of the ubiquitously expressed *UCP2* gene that had previously been implicated in this process (6, 7). Real-time PCR quantification of *UCP2* expression showed a significant increase (by 107%; $p < 0.01$) solely in affected individuals with G2019S LRRK2. In unaffected carriers, *UCP2* mRNA levels were comparable to those found in controls (Fig. 2A).

Next, to test whether the disease status in individuals with G2019S LRRK2 also correlates with the expression of the kinase activity augmenting mutant *LRRK2* allele (2), we quantified mRNA levels of c.6055G > A (p.G2019S) mutant *versus* wild-type *LRRK2* using mutation-specific primers in a real-time approach. This experiment showed comparable mutant-to-wild-type expression ratios in all individuals with the mutation and no expression of the mutant allele in the controls ($p_{unaffected} < 0.01$ and $p_{affected} < 0.05$; Fig. 2B).

Elevated levels of oxidative stress and autophagy markers only in affected G2019S mutation carriers

Since LRRK2 function has been linked to cellular redox state (2, 5) and mitochondrial clearance (8), we also investigated markers of mitochondrial content, oxidative stress, and autophagy. Western blot analysis using antibodies against the antioxidants cytosolic superoxide dismutase 1 (SOD1) and mitochondrial SOD2 showed elevated protein levels in some of the PD patients with the LRRK2 G2019S mutation. Interestingly, this effect was not seen in unaffected carriers of the same mutation.

To analyze autophagy in fibroblasts, we first determined cellular levels of p62 that is sequestered along with cytosolic cargo targeted for degradation by autophagosomes. Western blot analysis showed increased p62 levels only in PD patients with the *LRRK2 G2019S* mutation. Next, we quantified the conversion of cytosolic LC3-I into autophagosome-associated LC3-II. This experiment revealed a shift from LC3-I to LC3-II in the majority of affected individuals with G2019S LRRK2. Furthermore, we used an antibody against the mitochondrial protein GRP75 as a measure of mitochondrial mass. This approach indicated comparable mitochondrial content in all samples (Fig. 2C) despite the detected differences in mitochondrial copy number.

Conclusions and Future Directions

Although mutations in *LRRK2* are the most common known genetic cause of PD, the penetrance of the associated motor phenotype is far below 100% (3). The factors that trigger disease manifestation remain mostly elusive to date. One major reason for this is that there are currently no means to simulate the difference between affected and unaffected individuals harboring the same mutation *in vitro*. Respective studies exclusively rely on endogenous models, such as primary human cells from unaffected carriers and

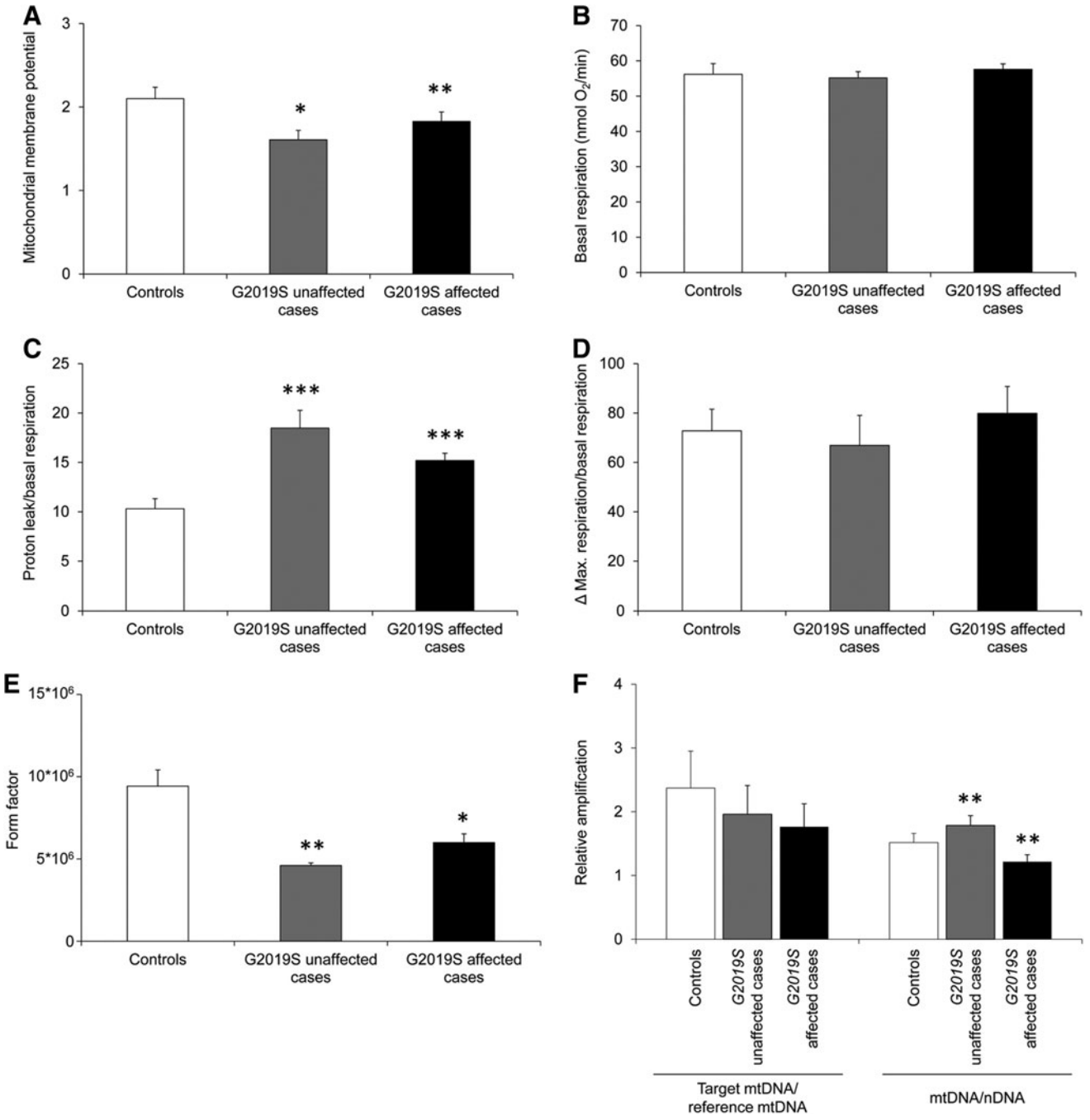

FIG. 1. Mitochondrial function and autophagy in fibroblasts from Parkinson's disease patients with LRRK2 G2019S mutation, unaffected carriers, and controls. **(A)** The mitochondrial membrane potential was significantly decreased in LRRK2-mutant fibroblasts from affected and unaffected individuals when compared with controls. **(B)** Oxygen consumption rates (OCRs) were assessed under basal conditions using an extracellular flux analyzer. This quantification showed comparable rates in all of the investigated groups. **(C)** The mitochondrial proton leak was determined after the addition of oligomycin and calculated relative to basal OCRs. The relative proton leakage was increased in all LRRK2 mutants independent of disease status. **(D)** Maximum respiration rates were detected after exposure to the mitochondrial uncoupler FCCP. When expressed relative to basal respiration, this treatment resulted in comparable ratios between groups. **(E)** Calculation of the form factor of the mitochondrial network (as a measure of interconnectivity) showed a decrease in both LRRK2-mutant groups of individuals. **(F)** Comparable target mtDNA to reference mtDNA ratios in LRRK2 G2019S mutants and controls indicated a similar degree of mtDNA lesions in the cells. The mtDNA-to-nuclear DNA (nDNA) ratio revealed an increase in the mtDNA copy number in the unaffected individuals and a decrease in the affected mutants when compared with controls. Bars represent mean values, and error bars represent the standard errors. $*p < 0.05$; $**p < 0.01$; $***p < 0.001$.

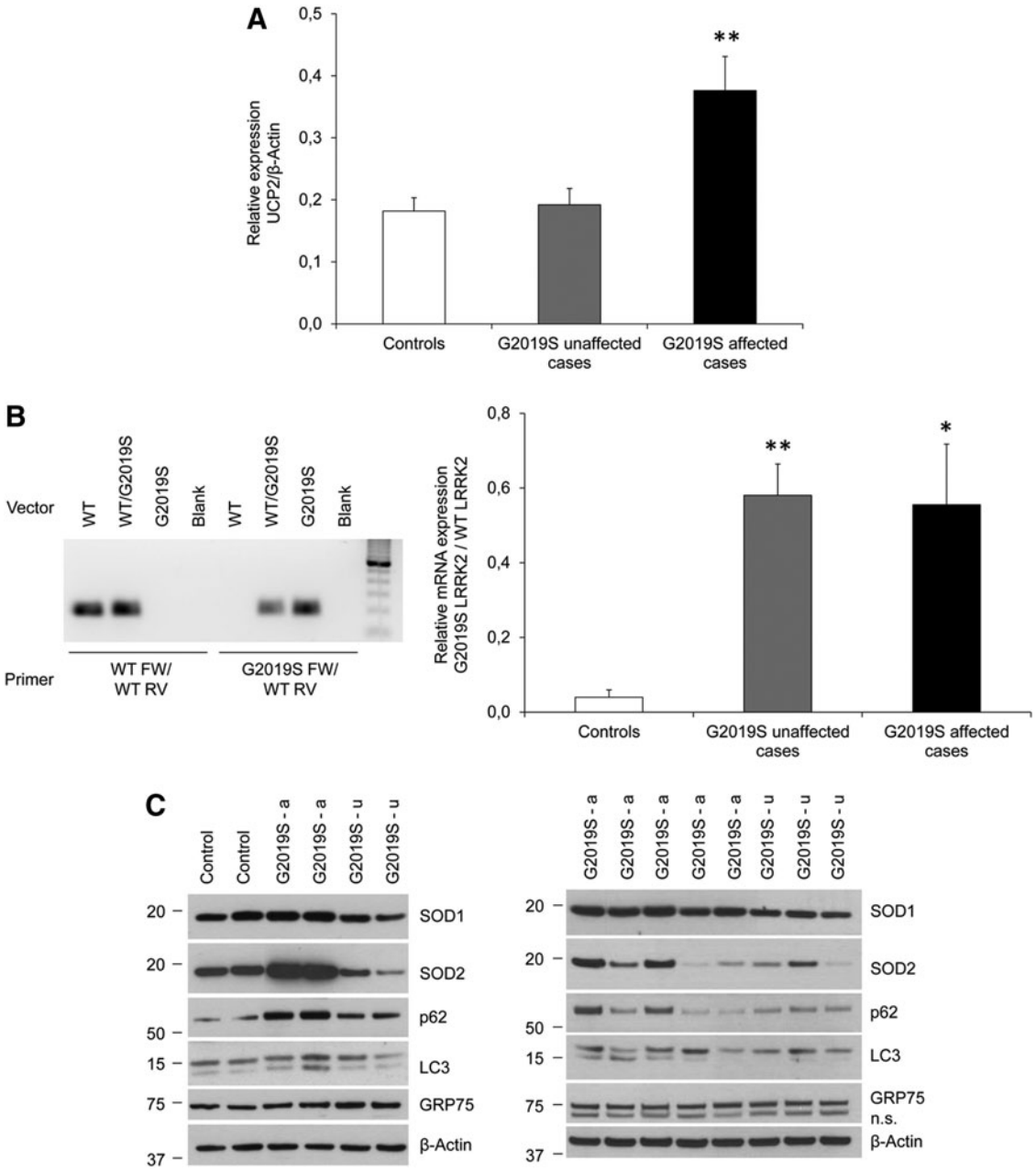

FIG. 2. Increased *UCP2* expression as a consequence of elevated cellular reactive oxygen species levels. (A) mRNA expression analysis of *UCP2* revealed normal levels in unaffected mutation carriers and an increase in affected G2019S LRRK2 mutants. **(B)** *LRRK2* expression analysis. A mutation-specific PCR was optimized to quantify wild-type (WT) *versus* c.6055G > A mutant *LRRK2* (G2019S LRRK2). Plasmids containing wild-type or c.6055G > A *LRRK2* cDNA sequences were used in a PCR reaction to verify the accuracy of amplification for primer pairs that were specific for wild-type *LRRK2* or c.6055G > A *LRRK2*. Resulting bands on an agarose gel were of the expected size (207 bp). Wild-type-specific primers selectively amplified wild-type *LRRK2* cDNA, whereas mutant-specific primers selectively amplified mutant *LRRK2* cDNA (*left panel*). Using the mutation-specific primers in a real-time approach, we determined comparable mutant-to-wild-type expression ratios in all of the mutation-positive samples (*right panel*). In both real-time assays, the target gene expression was normalized to the housekeeping gene *β-Actin*. **(C)** Protein expression of markers of oxidative stress and autophagy. Western blot analysis using antibodies against cytosolic SOD1, mitochondrial SOD2, p62, and LC3 showed increased SOD1 and SOD2 levels and a shift toward autophagosome-associated LC3-II in some of the affected individuals. Protein levels of the mitochondrial marker GRP75 indicate comparable mitochondrial mass in all individuals. *β*-Actin protein expression served as a loading control. Bars indicate mean values, and error bars represent standard errors. $*p < 0.05$; $**p < 0.01$; n.s., nonspecific.

mutation-positive patients. Following this line of thought and considering the established role of LRRK2 in mitophagy (8), we investigated parameters of mitochondrial and autophagosome function in fibroblasts from affected and unaffected individuals with the G2019S mutation in LRRK2. Our experiments identified mitochondrial uncoupling and fragmentation as phenotypes occurring not just in affected (4) but also in unaffected mutants. Interestingly, elevated mRNA expression of the mitochondrial uncoupler *UCP2* has recently been identified as the cause of mitochondrial proton leakage in fibroblasts with G2019S LRRK2 (6). In the current study, a detectable increase in *UCP2* mRNA levels was solely measured in cells from mutation-positive cases with PD, although the unaffected G2019S mutation carriers also presented with reduced mitochondrial membrane potential. Despite its genetic homology to UCP1, which contributes to adaptive thermogenesis by rapid and full uncoupling of respiration, the main function of UCP2 is to limit cellular reactive oxygen species (ROS) production by mild uncoupling of the respiratory chain (7). Therefore, we assume that the high expression of *UCP2* is provoked by elevated ROS levels in G2019S LRRK2-mutant PD patient cells. In support of our hypothesis, high protein levels of the antioxidants SOD1 and SOD2 were only detected in some of the PD patients but not in unaffected mutation carriers. This observation in conjunction with increased p62 or LC3-II levels in the same individuals may point toward blockage of autophagosome clearance as the ultimate cause of disease (8). In unaffected LRRK2 G2019S mutants, a slight (at the endogenous level undetectable) increase in *UCP2* expression may be sufficient to induce uncoupling as a successful countermeasure of increasing ROS. In such a scenario, the high *UCP2* expression seen in affected mutation carriers would be a result of the cell's ''lost battle'' against uncontrolled ROS generation. Another possible indicator of compensatory mechanisms in the unaffected mutants is the rise in mtDNA copy number. This increase may lead to enhanced generation of mtDNA-encoded proteins to maintain respiratory chain function despite the damaging effects of ROS.

Due to the small number of samples included in this study, our observation will require verification in a larger cohort to draw firm conclusions. Since the affected LRRK2 mutants had a higher average age than the unaffected mutation carriers, it cannot be fully excluded that aging contributes to the increase in *UCP2* expression. However, since elevated *UCP2* mRNA levels have earlier been observed in fibroblasts from LRRK2-mutant PD patients with a mean age of 55.8 ± 3.6 years but not in a control group with an about 13-year greater mean age (68.9 ± 4.8 years), the influence of age may be negligible (6). With regard to PD pathogenesis, investigations concerning the role of UCP2 in mitochondrial uncoupling and ROS scavenging would be more appropriate in neuronal cellular models, such as iPSC-derived patient neurons. Experiments in the much more vulnerable dopaminergic neurons are likely to yield even clearer differences between affected and unaffected LRRK2 mutants.

In summary, our results point toward a role of UCP2 as mild mitochondrial uncoupler protecting cells from ROS overload in *LRRK2*-associated PD. Therefore, the expression of the gene appears to correlate with disease status in G2019S LRRK2 mutation-positive individuals.

Notes

Materials and methods

Ethics statement. The study was approved by the ethics committee of the University of Lübeck, and all participants provided written, informed consent. All investigations in humans or human materials were conducted in conformity with the Declaration of Helsinki.

Patients. To generate fibroblast cultures, skin biopsies were taken from five PD patients with the G2019S mutation in LRRK2 (mean age: 65.4 ± 5.5 years, AAO: 61.4 ± 3.5, three female), three unaffected mutation carriers (mean age: 45.3 ± 9.2 years, three female), and four controls (mean age: 41.8 ± 6.4 years, two female) without mutations in known PD genes. All measurements were performed in at least three independent runs per individual.

Tissue culture. Fibroblasts were cultured in high-glucose Dulbecco's modified Eagle's medium that was supplemented with 10% fetal bovine serum and 1% penicillin–streptomycin (GE Healthcare, Little Chalfont, England) at 37°C, 5% CO_2. In all assays, fibroblast passage numbers (< 10) were matched.

Assessment of mitochondrial function. The mitochondrial membrane potential was determined using 5,5′,6,6′-tetrachloro-1,1′,3,3′-tetraethylbenzimidazolylcarbocyanine iodide (Invitrogen, Carlsbad, CA). To investigate OCRs (as an indicator of mitochondrial respiration), the Seahorse XF24, extracellular flux analyzer (Seahorse Bioscience, Copenhagen, Denmark) was employed using 60,000 fibroblasts per well. By this, the concentration of dissolved oxygen in the medium is measured in time intervals of 2 s by solid-state sensor probes. After determining the basal respiration in the cells, oligomycin (2 μM), FCCP (500 nM), and antimycin (3 μM) were sequentially added to the media and OCRs for each condition were quantified for two minutes (''BOFA'' experiment) (all Sigma, St. Louis, MO). Thus, respiration compensating for the mitochondrial proton leak, maximal respiration, and nonmitochondrial respiration were determined. The resulting rates were adjusted for protein concentration.

Real-time quantification of mitochondrial DNA stability and copy number. Quantitative PCR analysis was performed with the LightCycler DNA Master SYBR Green I kit on the Light Cycler 2.0 real-time PCR system (both Roche Diagnostics, Basel, Switzerland). The stability of mitochondrial DNA (mtDNA) was measured employing a semi-long run real-time approach. In brief, two mtDNA fragments of different length were amplified. A 55 bp reference fragment (primers: AS1.F/AS1.R) was used to monitor the total mtDNA concentration, and a 1037 bp target fragment (primers: DL1.F/DL1.R) served as an experimental probe to detect mtDNA lesions. In addition, total mtDNA levels were determined by measuring the 55 bp mtDNA fragment relative to the nuclear single copy gene *β-globin*.

Assessment of mitochondrial interconnectivity. The mitochondrial network was stained with an anti-GRP75 antibody (Abcam, Cambridge, England) and the zenon immunolabeling kit (Invitrogen) according to the manufacturer's protocol. Mitochondrial network morphology was investigated using a fluorescence microscope with an ApoTome (Zeiss, Jena,

Germany). Image analysis and calculation of the form factor (4) was performed using a self-designed macro in ImageJ 1.44. To study mitochondrial morphology, images of at least ten randomly selected cells were analyzed per individual.

Protein extraction and western blot analysis. Proteins were extracted using RIPA buffer containing 0.1% SDS (50 m*M* Tris-HCl pH7.6, 150 m*M* NaCl, 1% DOC, 1% NP-40, and 0.1% SDS). Fibroblasts were dissolved in the appropriate amount of buffer and incubated on ice for 30 min. Lysates were centrifuged at 16,000 *g* for 20 min at 4°C, and the supernatant was used for western blotting. SDS PAGE was performed using NuPAGE 4%–12% Bis-Tris gels (Invitrogen). After electrophoresis, proteins were transferred to a Protran nitrocellulose membrane (GE Healthcare) and probed with antibodies that were raised against SOD1 (Cell Signaling, Beverly, MA), SOD2 (Sigma), GRP75 (Cell Signaling), p62 (Cell Signaling), LC3 (Cell Signaling), and β-actin (Sigma).

mRNA expression analysis. For mRNA expression analysis of *LRRK2, UCP2* and *β-Actin* total RNA from fibroblasts was extracted using the RNA easy protect kit (Qiagen, Hilden, Germany) according to the manufacturer's instructions. Next, RNA was reverse-transcribed into cDNA with the Super Script First-Strand Synthesis System (Invitrogen). The resulting cDNA was investigated using real-time PCR employing the LightCycler DNA Master SYBR Green I kit on the Light Cycler 2.0 real-time PCR system (both Roche Diagnostics). For the allele-specific detection of *G2019S* and wild-type (WT) *LRRK2* expression, plasmids containing *WT LRRK2* or *c.6055G>A LRRK2* cDNA sequences served as standards. Primer sequences for all PCR reactions are available on request.

Statistical analysis. Means were plotted ± standard error of the mean (SEM), and significance was determined using a paired or nonpaired Student's *t*-test.

Acknowledgments

This study was supported by the Fritz Thyssen Foundation, a Habilitation Fellowship from the University of Lübeck, Germany, and research funding from the German Research Foundation.

References

1. Adams JR, van Netten H, Schulzer M, Mak E, McKenzie J, Strongosky A, Sossi V, Ruth TJ, Lee CS, Farrer M, Gasser T, Uitti RJ, Calne DB, Wszolek ZK, and Stoessl AJ. PET in LRRK2 mutations: comparison to sporadic Parkinson's disease and evidence for presymptomatic compensation. *Brain* 128: 2777–2785, 2005.
2. Cookson MR. The role of leucine-rich repeat kinase 2 (LRRK2) in Parkinson's disease. *Nat Rev Neurosci* 11: 791–797, 2010.
3. Healy DG, Falchi M, O'Sullivan SS, Bonifati V, Durr A, Bressman S, Brice A, Aasly J, Zabetian CP, Goldwurm S, Ferreira JJ, Tolosa E, Kay DM, Klein C, Williams DR, Marras C, Lang AE, Wszolek ZK, Berciano J, Schapira AH, Lynch T, Bhatia KP, Gasser T, Lees AJ, and Wood NW. Phenotype, genotype, and worldwide genetic penetrance of LRRK2-associated Parkinson's disease: a case-control study. *Lancet Neurol* 7: 583–590, 2008.
4. Mortiboys H, Johansen KK, Aasly JO, and Bandmann O. Mitochondrial impairment in patients with Parkinson disease with the G2019S mutation in LRRK2. *Neurology* 75: 2017–2020, 2010.
5. Nguyen HN, Byers B, Cord B, Shcheglovitov A, Byrne J, Gujar P, Kee K, Schule B, Dolmetsch RE, Langston W, Palmer TD, and Pera RR. LRRK2 mutant iPSC-derived DA neurons demonstrate increased susceptibility to oxidative stress. *Cell Stem Cell* 8: 267–280, 2011.
6. Papkovskaia TD, Chau KY, Inesta-Vaquera F, Papkovsky DB, Healy DG, Nishio K, Staddon J, Duchen MR, Hardy J, Schapira AH, and Cooper JM. G2019S leucine-rich repeat kinase 2 causes uncoupling protein-mediated mitochondrial depolarization. *Hum Mol Genet* 21: 4201–4213, 2012.
7. Rousset S, Alves-Guerra MC, Mozo J, Miroux B, Cassard-Doulcier AM, Bouillaud F, and Ricquier D. The biology of mitochondrial uncoupling proteins. *Diabetes* 53 Suppl 1: S130–S135, 2004.
8. Sanchez-Danes A, Richaud-Patin Y, Carballo-Carbajal I, Jimenez-Delgado S, Caig C, Mora S, Di Guglielmo C, Ezquerra M, Patel B, Giralt A, Canals JM, Memo M, Alberch J, Lopez-Barneo J, Vila M, Cuervo AM, Tolosa E, Consiglio A, and Raya A. Disease-specific phenotypes in dopamine neurons from human iPS-based models of genetic and sporadic Parkinson's disease. *EMBO Mol Med* 4: 380–395, 2012.
9. Vives-Bauza C, Zhou C, Huang Y, Cui M, de Vries RL, Kim J, May J, Tocilescu MA, Liu W, Ko HS, Magrane J, Moore DJ, Dawson VL, Grailhe R, Dawson TM, Li C, Tieu K, and Przedborski S. PINK1-dependent recruitment of Parkin to mitochondria in mitophagy. *Proc Natl Acad Sci USA* 107: 378–383, 2010.

Address correspondence to:
Dr. Christine Klein
Institute of Neurogenetics
University of Lübeck
Maria-Goeppert-Straße 1
Lübeck 23562
Germany

E-mail: christine.klein@neuro.uni-luebeck.de

Date of first submission to ARS Central, November 8, 2013; date of acceptance, November 18, 2013.

Abbreviations Used

DNA = deoxyribonucleic acid
FCCP = trifluorocarbonylcyanide phenylhydrazone
GRP75 = mortalin
iPSC = induced pluripotent stem cells
LC3 = microtubule-associated protein light chain 3
LRRK2 = leucine-rich repeat kinase 2
mtDNA = mitochondrial DNA
OCR = oxygen consumption rate
p62 = sequestosome 1
PD = Parkinson's disease
PINK1 = PTEN-induced putative kinase 1
RIPA = radio immunoprecipitation assay
RNA = ribonucleic acid
ROS = reactive oxygen species
SOD = superoxide dismutase
UCP = uncoupling protein